Laser speckle imaging with an active noise reduction scheme

A.C. Völker[1], P. Zakharov[1], B. Weber[2,3], F. Buck[2] and F. Scheffold[1]

[1]Department of Physics, University of Fribourg, 1700 Fribourg, Switzerland
[2]Division of Nuclear Medicine, University Hospital Zurich, Rämistrasse 100, 8091 Zurich, Switzerland
[3]Max Planck Institute for Biological Cybernetics, Spemannstraße 38, 72076 Tübingen, Germany
Andreas.Voelker@unifr.ch, Frank.Scheffold@unifr.ch

Abstract: We present an optical scheme to actively suppress statistical noise in Laser Speckle Imaging (LSI). This is achieved by illuminating the object surface through a diffuser. Slow rotation of the diffuser leads to statistically independent surface speckles on time scales that can be selected by the rotation speed. Active suppression of statistical noise is achieved by accumulating data over time. We present experimental data on speckle contrast and noise for a dynamically homogenous and a heterogeneous object made from Teflon. We show experimentally that for our scheme spatial and temporal averaging provide the same statistical weight to reduce the noise in LSI: The standard deviation of the speckle contrast value scales with the effective number N of independent speckle as $1/\sqrt{N}$.

©2005 Optical Society of America

OCIS codes: (110.6150) Speckle imaging; (170.7050) Turbid media; (170.3880) Medical and biological imaging; (110.4280) Noise in imaging systems.

References

1. J. D. Briers, "Laser Doppler and time-varying speckle: A reconciliation," J. Opt. Soc. Am. A **13,** 345 (1996).
2. J. D. Briers, "Laser Doppler, speckle and related techniques for blood perfusion mapping and imaging," Physiological Measurement **22,** R35-R66 (2001).
3. A. K. Dunn, B. Hayrunnisa, M. A. Moskowitz, and D. A. Boas, "Dynamic imaging of cerebral blood flow using laser speckle," J. Cereb. Blood Flow Metab. **21,** 195-201 (2001).
4. C. Ayata, Y. Ozdemir, A. Dunn, D. N. Atochin, P. L. Huang, V. R. Muzykantov, J. C. Murciano, D. A. Boas, and M. A. Moskowitz, "Laser speckle-flowmetry: A novel two-dimensional technique for the study of cerebral blood flow in normal and ischemic mouse brain, in vivo," Stroke **34,** 251-251 (2003).
5. H. Cheng, et. al., "Modified laser speckle imaging method with improved spatial resolution," J. Biomed. Opt. **8,** 559-564 (2003).
6. B. Weber, C. Burger, M. T. Wyss, G. K. von Schulthess, F. Scheffold, and A. Buck, "Optical imaging of the spatiotemporal dynamics of cerebral blood flow and oxidative metabolism in the rat barrel cortex," Eur. J. Neurosci. **20,** 2664-2670 (2004).
7. B. J. Berne, and R. Pecora, *Dynamic Light Scattering* (John Wileys and Sons, New York, 1976).
8. R. Bandyopadhyay, A. S. Gittings, S. S. Suh, P.K. Dixon, and D. J. Durian, "Speckle-visibility spectroscopy: A tool to study time-varying dynamics," Rev. Sci. Instrum. **76,** art. no. 093110 (2005).
9. J. C. Dainty, *Laser speckle and related phenomena* (Springer-Verlag, Berlin ; New York, 1984).
10. L. F. Rojas, D. Lacoste, R. Lenke, P. Schurtenberger, and F. Scheffold, "Depolarization of backscattered linearly polarized light," J. Opt. Soc. Am. A **21,** 1799-1804 (2004).
11. E. Jakeman, and E. R. Pike, "Intensity-fluctuation distribution of Gaussian Light," J. Phys. I **1,** 128-138 (1968).
12. J. D. Briers, and S. Webster, "Laser speckle contrast analysis (LASCA): A nonscanning, full-field technique for monitoring capillary blood flow," J. Biomed. Opt. **1,** 174-179 (1996).
13. F. C. Mackintosh, J. X. Zhu, D. J. Pine, and D. A. Weitz, "Polarization memory of multiply scattered-light," Phys. Rev. B **40,** 9342-9345 (1989).
14. T. Yoshimura, and K. Fujiwara, "Statistical properties of doubly scattered image speckle," J. Opt. Soc. Am. A **9,** 91-95 (1992).
15. D. J. Pine, D. A. Weitz, P. M. Chaikin, and E. Herbolzheimer, "Diffusing-wave spectroscopy," Phys. Rev. Lett. **60,** 1134-1137 (1988).
16. L. Cipelletti, and D. A. Weitz, "Ultralow-angle dynamic light scattering with a charge coupled device camera based multispeckle, multitau correlator," Rev. Sci. Instrum. **70,** 3214-3221 (1999).

17. P. Zakharov, S. Bhat, P. Schurtenberger, and F. Scheffold, "Multiple scattering suppression in dynamic light scattering based on a digital camera detection scheme," Appl. Opt. in press, (2005).
18. P. N. Pusey, and W. Vanmegen, "Dynamic light-scattering by Non-Ergodic Media," Physica A **157,** 705(1989).
19. F. Scheffold, S. E. Skipetrov, S. Romer, and P. Schurtenberger, "Diffusing-wave spectroscopy of nonergodic media," Phys. Rev. E **6306,** art. no. 061404 (2001).
20. T. Yoshimura, "Statistical properties of dynamic speckles," J. Opt. Soc. Am. A **3,** 1032-1054 (1986).
21. S. E. Skipetrov, and I. V. Meglinskii, "Diffusing-wave spectroscopy in randomly inhomogeneous media with spatially localized scatterer flows," J Exp. Theor. Phys. **86,** 661-665 (1998).
22. A. C. Völker, P. Zakharov, B. Weber, A. Buck, and F. Scheffold, "Dynamic contrast resolution in laser speckle imaging," in preparation (2005).
23. S. Yuan, A. Devor, D. A. Boas, and A. K. Dunn, "Determination of optimal exposure time for imaging of blood flow changes with laser speckle contrast imaging," Appl. Opt. **44,** 1823-1830 (2005).

1. Introduction

Laser speckle imaging (LSI) [1-6] is an optical technique that can be used to measure local dynamic properties in scattering media both at high temporal and spatial resolution. The underlying principle of LSI is equivalent to the one exploited in laser Doppler flowmetry (LDF), a method widely used in biomedical functional imaging of blood flow [2]. A moving object inside the tissue, such as a red blood cell, leads to a Doppler shift of the frequency of scattered light which is directly proportional to the velocity. Rather than analyzing Doppler frequency shifts LSI monitors temporal fluctuations of the scattered light in order to map dynamics. From a fundamental point of view both techniques are equivalent [1]. The frequency and time domain in quasi-elastic light scattering are connected by a simple Fourier transformation and thus completely interchangeable (Wiener-Khinchin theorem) [2, 3, 7, 8]. In other words if the spectrum of frequency shifts is known the distribution of temporal fluctuations can be calculated and vice versa. In LSI a digital camera records the surface intensity pattern of light reflected from a scattering medium. In the absence of movement (or for very short exposure time) there is no detectable fluctuation and the typical granular interference pattern, called speckle, has the same properties in the entire field of view. In the classical picture, summarized by Goodman in [9], the scattered field amplitudes are randomly distributed and consequently the intensity values follow a negative exponential distribution $P(I)\langle I \rangle = \exp(-I/\langle I \rangle)$. In an experiment the normalized standard deviation (or contrast) is:

$$K = \beta \langle I \rangle^{-1} \left[\sum_{i=1}^{N} \left(I_i - \langle I \rangle \right)^2 \Big/ N - 1 \right]^{1/2}. \tag{1}$$

Here we have additionally introduced the so called coherence factor β that takes account of the finite size of the detection area and depolarization of light in the medium [10]; it approaches 1 only using a polarization filter and a point detector. For a fully developed static speckle $K = \beta$. Changes in the position of some objects lead to temporal intensity fluctuations with a time constant given by the local velocity. Such time fluctuations are usually characterized by the normalized intensity autocorrelation function $C(\tau) = \langle I(0)I(\tau) \rangle / \langle I \rangle^2 - 1$. Instead of analyzing the temporal fluctuations in detail it is more convenient to measure a time averaged quantity simply by choosing a certain camera exposure time T. Then the average speckle contrast decreases according to $K = \beta/T \int_0^T 2(1 - t/T) C(\tau) d\tau$. For a simple exponential decay $C(\tau) = \exp(-\tau/\tau_c)$ one finds [8], [11]:

$$K = \beta \int_0^T 2(1 - t/T) C(\tau) d\tau / T = \sqrt{\beta \frac{e^{-2x} - 1 + 2x}{2x^2}} \quad with \quad x = \frac{T}{\tau_c}. \tag{2}$$

The spatially resolved speckle contrast K is a sensitive probe of the dynamic properties. High contrast corresponds to slow movement while low contrast is found in areas of fast movement. In other words areas with motion "blur" the speckle pattern while static areas do

not. In the so called Laser Speckle Contrast Analysis (LASCA) [12] approach an image is obtained from a simple analysis of the variance in a small area of typically $N = 5x5 = 25$ or $N = 7x7 = 49$ pixels. As a matter of fact calculation of the speckle contrast is limited to such small areas of a few pixels if a high spatial resolution is desired. We will call this area in the following "square size". The choice of the square size is a compromise between statistical accuracy and spatial resolution. In such LASCA imaging the statistical noise is naturally very high, typically around $N^{-0.5} \sim 15\text{-}20\%$ for a non-averaged single frame image.

2. Active noise reduction scheme

It would thus be of particular interest to find ways of improving the statistical accuracy without loss in spatial resolutions. A first step in this direction has been reported recently by Cheng et al. [5]. The authors suggest a temporal speckle averaging scheme implicitly assuming that subsequent speckle images are more or less statistically independent. Calculating the speckle contrast from a series of intensity values recorded at the same position an image can be constructed without loss in spatial resolution. The fact that this method gives meaningful results is somewhat fortuitous as we will discuss below.

Here we propose a more rigorous approach to noise reduction based on an active speckle averaging scheme that ensures perfect ensemble averaging. The basic idea is to illuminate the sample with a random speckle field which can be varied externally using a rotating diffuser. Rather than using an expanded collimated beam the sample surface is illuminated with a dispersed laser beam that has passed a ground glass. The resulting divergent beam creates an effective speckle illumination on the sample surface placed at a distance of $z = 20$ cm with a corresponding surface speckle size of $\lambda z/\pi w \sim 25$ µm for an incident beam size of approximately $w = 2$ mm. Slowly rotating the ground glass leads to statistically independent realizations of the speckle pattern with characteristic temporal fluctuations on a time scale τ_0 which can be controlled externally by the motor speed. If τ_0 is chosen much larger than the desired exposure time T of the digital camera, subsequent speckle images taken at time intervals larger τ_0 are statistically independent. Analyzing a larger number N of images this method allows perfect statistical averaging of the contrast without any spatial averaging. Thus the full resolution of the speckle image is preserved. It is worthwhile to note that for a freely propagating laser beam a similar effect could be achieved by moving the sample or the laser, which is however much less practical.

3. Experiments and results

To explore the range of applications of the method and to illustrate the noise reduction we study the dynamic contrast resolution using a homogeneous block of solid Teflon and a home-made heterogeneous sample. This medical phantom mimics a liquid inclusion in solid tissue. It is obtained by milling a cylindrical hole of diameter $D_0 = 3$ mm in a block of solid Teflon. A thin layer of 0.45 mm (accuracy 0.01 mm) separates the cylindrical inclusion from the interface that is imaged. The void is subsequently filled with a dispersion of 710 nm polystyrene particles in water. The particle concentration is adjusted to match the optical properties of the liquid to the solid (volume fraction ca. 1.3%). Thus our sample does not show any static scattering differences (Fig. 1).

A diode laser beam (785 nm, max. 50 mW) is incident on a ground glass (Edmund Optics), which is mounted on a motor. Light passing the ground glass is dispersed and illuminates the sample surface as an expanded light spot. The illuminated surface is then imaged with a camera objective (Schneider Kreuznach Xenoplan, $f = 50$ mm, distance lens-image plane $l = 80$ mm) onto the CCD chip of a digital camera (Pixelfly PCO, Germany). The camera resolution is 640x480 pixels (edge length of pixel $r_P = 9.9$ µm, half inch chip) and with our camera objective the full field of view is 16 by 12. A crossed linear polarizer is set in front of the objective to eliminate spurious contributions from reflections and to increase the speckle contrast [13]. To correct for slightly inhomogeneous illumination we have divided the intensity value of each pixel by its mean (taken from 500 statistically independent

measurements). In practice this only affects the results for square sizes 16x16 or larger, while for all others there is no notable difference with or without normalization.
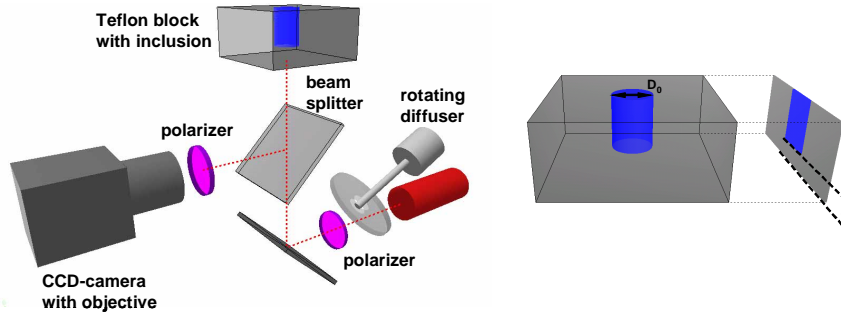

Fig. 1. Experimental setup: A laser beam (785 nm) is incident on ground glass mounted on a motor (rotation velocity one rph). Light passing the ground glass is moderately divergent and illuminates the sample surface as an expanded light spot. The illuminated surface is imaged via a beam-splitter by the camera objective onto the CCD chip of the digital camera. Right: Heterogeneous sample obtained by milling a cylindrical void (diameter $D_0 = 3$ mm) into a solid block of Teflon. The inclusion is filled with an aqueous suspension of 710 nm polystyrene latex spheres that matches the optical properties ($l^*=250\pm30$ µm) and creates dynamic contrast. A layer of thickness d = 0.45 mm separates the inclusion from the imaging surface.

Due to scattering and de-phasing in the ground glass the light spot on the surface displays a fully developed speckle pattern [14]. In the presence of the turbid media the characteristic surface speckle pattern is seen. This pattern is basically the same whether the beam is expanded by a lens or by the ground glass. As a matter of fact we expect no influence of the random diffuser on the surface speckle as long as the distance travelled by the light inside the sample is larger than the size of a surface speckle created by the diffuser. In our case this surface speckle size is approx. 25 µm and the typical distance travelled by the light is the transport mean free path ($l^*=250\pm30$ µm for Teflon and the colloidal suspension, as determined by diffusing wave spectroscopy [15]).

It is worthwhile to emphasize the marked difference to previous temporal-averaging schemes [5]. In our case the noise reduction is "active". Every single image taken is statistically independent from the previous one. Passive time averaging schemes on the other hand rely on experimental noise such as animal motion or other slow fluctuations that are beyond the control of the operator. Furthermore, the method proposed by Cheng et al. [5], is actually very similar to the empiric approach to average over a couple of images taken within a short time interval where the dynamics of the system (such as cerebral blood flow) can be assumed stationary [3, 6]. It is well known from digital camera based intensity correlation spectroscopy that in the limit of large numbers N the so called "divide and average scheme" provides the same results as the "average and divide" scheme [16, 17]. Time averaging in both cases however relies on the ergodicity of the medium (the possibility to obtain ensemble averages by time averaging) [18, 19]. In practice this means that consecutive pictures have to be statistically independent. This is only the case if the correlation function of each pixel $C_{i,j}(\tau)$ has relaxed to zero between the acquisition of two images. Whether this is the case or not however depends on the camera frame rate and the unknown temporal behavior of $C_{i,j}(\tau)$ which furthermore is different for each position (pixel i,j). In regions of slow or arrested decay of $C_{i,j}(\tau)$ the above mentioned approaches do not improve the statistical accuracy at all: averaging subsequent recordings of basically time independent speckle does not reduce noise. For a well controlled model experiment, as in the case of our Teflon phantoms, simple time averaging will add little or no statistical weight since the static part of the recorded speckle pattern does not fluctuate at all.
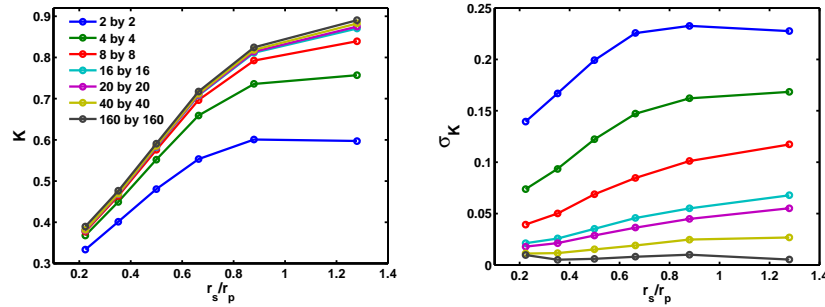
Fig. 2. Characteristics of the laser speckle imaging setup obtained from a rigid sample (Teflon block) for different LASCA square sizes. a) mean speckle contrast K as a function of the speckle size (in units of the pixel size r_P). b) Standard deviation of the contrast σ_K as a function of r_S. To achieve approximately the same intensity for all apertures the exposure time was varied between 200 and 750 ms.

Some characteristics of our laser speckle imaging device are displayed in Fig. 2. A single image was taken for different imaging apertures from the homogeneous rigid Teflon block. The corresponding f-number ($f/\#$) is the focal length f divided by the radius q of the aperture. The speckle size r_s on the CCD is then equal to [20]:

$$r_s = 2l/k_0 q = 4 \times f/\# \times l/k_0 f .\qquad(3)$$

Here l is the distance of the image to the lens and k_0 is the wave number. The mean speckle contrast K and the contrast noise σ_K are shown for different box sizes. With increasing f-number the speckle size is increased and thus the mean contrast increases approaching the limit of a point detector $r_S \gg r_P$. At the same time the contrast noise increases since the number of speckle per area decreases (intensities on neighbouring pixels are more correlated). For all other experiments shown in this study we use $f/\# = 16$ with a corresponding speckle size $r_s = 12.8\ \mu m$, which is comparable to our CCD pixel size.
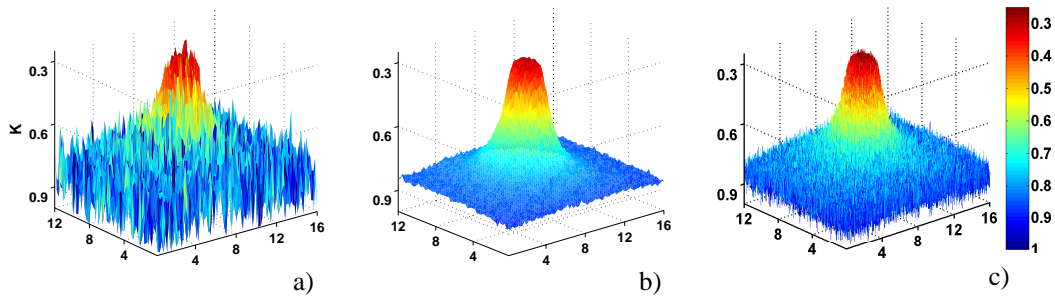

Fig. 3. Three dimensional plot of a laser speckle contrast image of a liquid inclusion in a solid block of Teflon (scale inverted). a) LASCA image using 8x8 square size, image resolution 80x60 pixel averaged over 500 individual measurement. b) Same sample using the active noise reduction. c) Full resolutions 640x480 pixel with active noise reduction scheme.

To study the dynamic resolution in the speckle image we first apply the traditional LASCA scheme using a 8x8 square size. As can be seen in Fig. 3(a) the contrast significantly decreases at the location of the liquid inclusion and in the near vicinity, overall however the signal remains very noisy. As shown in Fig. 3(b) a strikingly improved picture appears if we rotate the ground glass slowly with approximately one rotation per hour and construct an image from a series of images. At the selected motor speed the relaxation time has been determined to $\tau_0 = 450$ ms. 500 images were taken with 1 fps. Thus the time interval between the single frames is larger then τ_0, corresponding to $N = 500$ statistically independent

measurements. For a full resolution dynamic image (640x480 contrast values *K*) the noise level can thus be estimated to $1/\sqrt{N} = 4.5\%$ as compared to the 20% error in the 8x8 square size LASCA experiment at only 80x60 resolution. A comparison is shown in Fig. 3.

We have performed a systematic study of the contrast noise for the case of a solid Teflon block. Since subsequent images are statistically independent, rotation introduces a "third dimension" in our averaging scheme. In principle it should be of no importance whether the *N* pixels used to calculate the contrast *K* are taken along the x, y or t-axes. Experimentally we indeed find that the noise in speckle contrast, characterized by its standard deviation $\sigma_K = \sqrt{\sum_{i=1}^{N}(K_i - <K>)^2/(N-1)}/<K>$ scales with $1/\sqrt{N}$ and $N = x \cdot y \cdot \#/\ frames$ as long as *N* is sufficiently large (*N* >100) as shown in Fig. 4. For *N* > 10000 the noise level saturates at a level well below 1%. We speculate that in this regime other sources of error become sizable such as spurious contributions of light not randomized by the diffuser, the inherent noise level of the CCD camera, fluctuations of the laser intensity or the beam point as well as contributions from ambient light or reflections at the optical elements. Since the noise level is already very low for all practical means we have not further elaborated on this question.
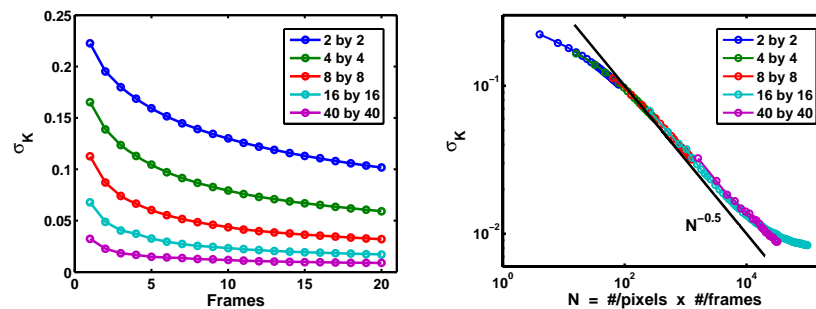

Fig. 4. Left: Noise in speckle contrast, expressed by the standard deviation σ_K, as a function of the number of frames taken, different square sizes are displayed (where #/*pixel* is the number of pixels in the corresponding square size). b) σ_K scaling as a function of "effective pixels" *N*. It is shown that spatial and temporal averaging give identical results.

4. Summary and conclusions

In summary we could demonstrate that our experimental scheme can efficiently suppress noise in LSI. Down to noise levels below 1% the accuracy that can be achieved is only limited by the total time of data acquisition. For a model experiment, as shown in the present examples, this time can be made arbitrarily long – leading to significant noise reduction as shown in Fig. 3(b),and 3(c). Such improved accuracy in model experiments should turn out to be very useful in the theoretical and experimental discussion of general principles of light propagation and imaging in turbid media [21, 22]. In a practical biomedical application the number of images that can be acquired will be limited by the time available in an experiment. In a typical case using a camera with 200 fps (frames per second) and with a reasonable exposure time of 1 ms [23], our approach can provide 40 independent images within 0.2 seconds, sufficient to follow physiological change in real time [6]. If combined with a moderate spatial average of 3x3 pixels the noise level can be reduced to approximately 5% over the full field of view. Note that the traditional LASCA spatial averaging scheme would require 20x20 pixels to achieve the same statistical accuracy. We thus believe that our technically very simple scheme also offers significant advantages for practical implementations of LSI in biomedical imaging.

Ackowledgments